USE OF THE ZONAL HARMONIC SERIES FOR OBTAINING NUMERICAL SOLUTIONS TO ELECTROMAGNETIC BOUNDARY VALUE PROBLEMS

Richard L. Lewis
Office of Telecommunications
U. S. Department of Commerce
Institute for Telecommunication Sciences
Boulder, Colorado 80302

This is a discussion of the application of the zonal harmonic series to problems involving dipole sources in the vicinity of spherical boundaries. The application of a formal zonal-harmonic series solution to directly obtain numerical results involves two distinct problems: namely, the convergence of the series solution and the accurate calculation of the special functions involved in the series solution. Some interesting techniques will be introduced which help to improve the convergence properties of the series solution.

Introduction

The numerical techniques involved will be discussed in light of two distinct problems for which numerical summation of the zonal-harmonic series is especially applicable. In the first problem, we are interested in calculating the magnetic field wave-tilt on the surface of a spherical hill due to a buried magnetic dipole orientated in a vertical direction off of the axis of symmetry, as illustrated in figure 1. This problem has application to locating the position of a buried magnetic dipole source in hilly terrain from surface measurements of the field. The major distinction of this problem is that the spherical Bessel functions involved in the formal series solution all have complex arguments, of which more will be said later. The formal solution of this problem proceeds, incidentally, by summing the zonal harmonic series solution for an inclined dipole source and then performing a rotation of coordinates to allign the dipole axis with the vertical. This leads to the interesting problem of relating the spherical coordinate θ' of the rotated sphere to the horizontal distance between two surface points that grow further apart (the distance X in figure 1) such that the bearing ψ from the source to the observer remains constant. Another problem of note is to obtain the magnitude and phase of the maximum component of the field in the horizonal plane when the two component fields are not necessarily in phase.

The second problem of interest is the application of the zonal harmonic series to the calculation of the fields in the earth-ionosphere waveguide due to a dipole source on the earth's surface. In the preceeding problem, the frequency range is restricted to low enough values so that the zonal harmonic series was a natural consideration, and so it is also in the case of the earth-ionosphere waveguide for frequencies in the ELF or lower part of the VLF range. Nevertheless, it is frequently felt by many that the mode series solution is preferable for physical interpretation as well as for simplicity of computation. The former point cannot be argued, but the latter point is only valid when it is possible to oversimplify the problem, say by assuming the ionosphere reflection coefficient is nearly unity. When more realistic assumptions about the upper boundary are made, a mode theory solution requires a search for modes by some sort of iterative process[1], which can be more time consuming than summing the series solution. One interesting analytical step that is utilized by both the contour integral formulation as well as zonal harmonics is to expand the denominator for each component of the series in a geometric series and then interchange the order of summation.[2] This has the advantage for mode theory that the ionosphere term is removed from the residue calculation, while for zonal-harmonics the convergence of the series is greatly improved. In each case, the outer series has the physical interpretation of wave-guide hops for which the series converges rapidly for VLF frequencies on up.

In the discussion of these two applications, the convergence of the series has been alluded to numerous times. Generally speaking, adequate convergence of the amplitude of the zonal harmonic series is attained by summing $10 \times ka$ terms, where $k = \frac{2\pi}{\lambda}$ is the wave number and a is the radius of the spherical boundary.[3] Adequate convergence of the phase usually requires a 50% increase over that number of terms. A few techniques have been utilized to make minor improvements in the speed of convergence, such as noting that the Legendre polynomial is a cyclic function of the summation index and consequently selective grouping of the terms produces partial sums which can be averaged to give some improvement. However, the major technical problem is the calculation of the special functions, using recursion formula. The Legendre polynomial is well behaved,[4] but not so the spherical Bessel functions. One spherical Bessel function increases asymptotically with the summation index, while the other decreases asymptotically. Consequently the functions must always be paired to avoid exponential underflow or overflow problems on the machine. This can involve some additional problems in arranging the Bessel functions as components in each term of the formal series solution. For the case of the Bessel function which decreases asympotically with the index of summation, backward rather than forward recursion must be utilized. How far backwards one must recurse is always a problem, but for the case of Bessel functions of complex argument it is of significant practical interest to note that the starting point need not be at an order which exceeds the magnitude of the argument, as is necessary for Bessel functions of real argument.[5] This is of particular importance for calculating the fields below the surface, since there the wave number may be much greater than the free space wave number, with the consequence that the argument of the spherical Bessel function can be quite large. Fortunately, the calculation of the Bessel functions by recursion is not only fast but produces very accurate results since, for both forward and backward recursion, the numerical process converges naturally to the desired function.

Buried Magnetic Dipole Model

Having thus introduced the range of our investigation, we can proceed with introducing explicit expressions for a buried magnetic dipole in a spherical hill.

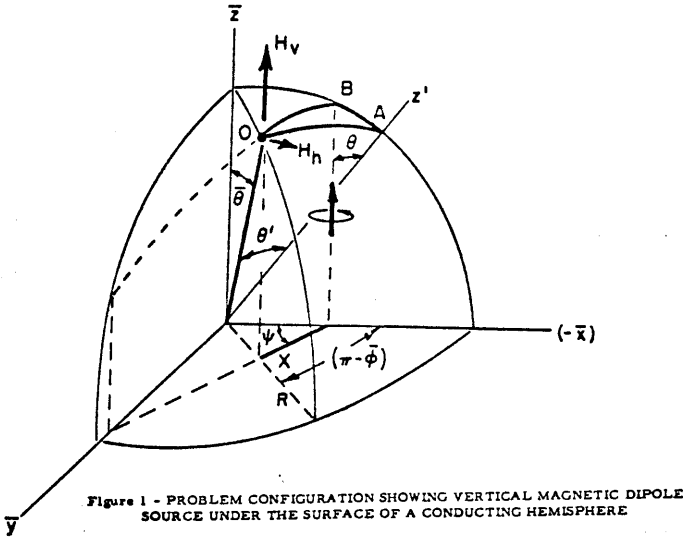

Figure 1 - PROBLEM CONFIGURATION SHOWING VERTICAL MAGNETIC DIPOLE SOURCE UNDER THE SURFACE OF A CONDUCTING HEMISPHERE

In figure 1 the z' axis forms a part of a rotated (x', y', z') coordinate system. The x' axis subtends an angle θ with the $\bar{x}$ axis, where θ is the dipole tilt angle. The y' and $\bar{y}$ axes are coincident. The corresponding spherical coordinates in the rotated coordinate system are R, θ', and φ', where the latter angle lies in a plane perpendicular to the z' axis. The formal series solution for the magnetic field components can easily be expressed in the rotated coordinate system. For convenience we introduce the abbreviations

$$\alpha = \cos\theta \qquad \beta = \sin\theta \ .$$

Thus, those terms multiplied by α denote the contribution to the fields due to the source component orientated along the z' axis, while those terms multiplied by β denote the contribution from that source component orientated parallel to the x' axis. The series solution for the component fields at the surface of the spherical hill is given by

$$H_R = \frac{\alpha R}{R_o}\sum n(n+1)(2n+1)\,P_n(\cos\theta')a_n - \beta\cos\phi'\sum(2n+1)\,P_n^1(\cos\theta')\frac{b_n}{u_n}$$

$$H_{\theta'} = \frac{\alpha R}{R_o}\sum(2n+1)\,P_n^1(\cos\theta')a_n\,u_n - \beta\cos\phi'\sum\frac{2n+1}{n(n+1)}\left[\frac{\partial P_n^1(\cos\theta')}{\partial\theta'}b_n + \frac{P_n^1(\cos\theta')}{\sin\theta'}c_n\right]$$

$$H_{\phi'} = \beta\sin\phi'\sum\frac{2n+1}{n(n+1)}\left[\frac{P_n^1(\cos\theta')}{\sin\theta'}b_n + \frac{\partial P_n^1(\cos\theta')}{\partial\theta'}c_n\right] \ , \qquad (1)$$

where R is the radius of the spherical hill (c.f. figure 1), R_o is the radial distance to the dipole source, the index of summation is n, $P_n(X)$ is the Legendre polynomial of order n, the associated Legendre function is $P_n^1(\cos\vartheta) = \frac{\partial}{\partial\vartheta}P_n(\cos\vartheta)$, and we have

$$a_n = \frac{\psi_n(k_1R_o)}{\psi_n(k_1R)}/D_n \qquad b_n = k_1R\frac{\psi_n'(k_1R_o)}{\psi_n(k_1R)}\times u_n/D_n \ , \qquad (2)$$

$$c_n = \frac{\psi_n(k_1R_o)/\psi_n(k_1R)}{u_n - \frac{k_2^2R}{k_1}\ln'\left[\psi_n(k_1R)\right]}\times(k_2R)^2 \ , \qquad (3)$$

where

$$D_n = u_n - k_1R\ln'\left[\psi_n(k_1R)\right] \qquad (4)$$

and

$$u_n = k_2R\ln'\left[\zeta_n^{(2)}(k_2R)\right] = k_2R\frac{\zeta_n^{(2)\prime}(k_2R)}{\zeta_n^{(2)}(k_2R)} \approx -n \ . \qquad (5)$$

In the above, $\psi_n(x)$ is the spherical Bessel function of the first kind and $\zeta_n^{(2)}(x)$ is the spherical Hankel function of the second kind, the primes on the spherical Bessel functions denote differentiation with respect to the argument in parenthesis, k_1 is the complex wave number for propagation in the media inside the spherical hill, and k_2 is the free space wave-number exterior to the spherical hill. The dipole magnetic current normalization is $J_m d\ell = -j\omega\mu_o R_o A$, where A is the surface area of the sphere. Those terms in equations (1) containing a_n and b_n constitute contributions from the scalar magnetic potential, while those terms containing c_n are contributions from the scalar electric potential.

The summations indicated in (1) receive their maximum contribution from terms of the order of $n \approx |k_1R|$. For orders of n much larger than this, we have $D_n \sim -2n$ and $\psi_n(k_1R_o)/\psi_n(k_1R) \sim (\frac{R_o}{R})^n$. Consequently, we can expect the magnitude of subsequent terms to decrease very rapidly. Moreover, if terms of order very much less than $|k_1R|$ are removed from the summation there is negligible effect on the summation value. This, in conjunction with the fact that k_2R is quite small in most problems of interest, leads to the validity of the approximation in (5). Moreover, the contribution from the scalar electric potential term (3) can be expected to be small, so that to a first approximation the only term involving frequency in the expressions for the field is k_1R. Consequently, it can be anticipated that the ratio of the source depth to skin depth, $H = \sqrt{\omega\mu_o\sigma}\times d$, where d is the depth below point B to the source, is a significant parameter of the problem.

We can introduce the following asymptotic formula for the Legendre function,

$$P_n(\cos\theta) \sim \frac{2\cos\left[(n+\frac{1}{2})\theta - \pi/4\right]}{\left[2\pi(n+1)\sin\theta\right]^{\frac{1}{2}}} \ , \qquad (6)$$

which provides us with a suggestive means for grouping terms of the summation in order to improve the convergence properties of the series.[3] Viewed as a function of the summation index n, equation (6) is nearly periodic of period $\frac{2\pi}{\vartheta}$. Consequently, terminating successive partial sums when the Legendre function changes sign and averaging only even numbers of such partial sums is equivalent to integrating (6) with respect to n over the period.

The practical question to be answered is how many terms are required for graphical accuracy. This is obviously a function of the ratio R_o/R as well as the value of $|k_1R|$. Assuming that R_o/R is nearly unity and that the elevation angle of the observation point ϑ' lies well away from the extreme positions zero or pi, then the summation can be truncated at $n \approx 10|k_1R|$ with negligible effect on the value of the summation from the neglected terms. It should be pointed out, however, that for very small angles ϑ' the number of terms required for convergence increases drastically (unless the ratio R_o/R is much less than unity).

The calculation of the special functions involved in the summation proceeds by invoking the recursion formu- for each special function required. Thus the series summation and the special function calculation are able to proceed rapidly together. The recursion formula for the Legendre polynomial is

$$P_{n+1}(x) = \frac{(2n+1)\,x\,P_n(x) - n\,P_{n-1}(x)}{n+1} \quad ,$$

$$P_0(x) = 1 \quad \text{and} \quad P_1(x) = x \quad . \tag{7}$$

This recursion process, as well as related formulas for the derivatives of the Legendre function, absolutely converges to the required functional values.* The calculation of the logarithmic derivative of the spherical Hankel function is also readily accomplished using foward recursion.[5] The spherical Bessel function of the first kind, however, requires use of a backwards recursion formula and careful attention to the problem of computer underflow. The backwards recursion relation for the logarithmic derivative is

$$\frac{\psi_{n-1}'(x)}{\psi_{n-1}(x)} = \frac{n}{x} - \frac{1}{\frac{n}{x} + \frac{\psi_n'(x)}{\psi_n(x)}} \quad , \quad n \le n_s \tag{8}$$

The starting value of the index n_s need only be slightly larger than the value of the index n required in the series summation when $n \ge |z|$. For n significantly less than $|z|$, where the argument of z is large, then a starting value $n_s \approx \frac{|z|}{2}$, say, would be sufficient[5] to generate functional values when $n \le \frac{|z|}{5}$, $|z| \ge 1000$. On the other hand, if z is real, then a starting value $n_s > z$ is required at all times. The initial value of the logarithmic derivative is arbitrarily chosen to be zero for the backward recursion process.

Using the value of the logarithmic derivative, the ratios of two spherical Bessel functions of the first kind with different arguments can be obtained from the relations

$$\frac{\psi_n'(x)}{\psi_n(x)} = -\frac{n}{x} + \frac{\psi_{n-1}(x)}{\psi_n(x)} \tag{9}$$

and

$$\frac{\psi_n(x)}{\psi_n(y)} = \frac{\psi_n(x)}{\psi_{n-1}(x)} \times \frac{\psi_{n-1}(x)}{\psi_{n-1}(y)} \times \frac{\psi_{n-1}(y)}{\psi_n(y)} \quad . \tag{10}$$

The starting value for (10) is given by

$$\frac{\psi_0(x)}{\psi_0(y)} = \frac{\sin x}{\sin y} \quad . \tag{11}$$

Thus, by restricting our calculations to the ratios of the Bessel functions, we have avoided the numerical underflow problem.

The wave tilt of the magnetic-field at an observation point on the surface of the spherical hill is defined as the ratio of the maximum horizontal field component to the vertical field component, where the vertical direction coincides with the direction of the magnetic dipole current moment. Two complex components in the horizontal plane combine to form the maximum horizontal component, which lies at some unknown angle γ in the horizontal $\bar{x} - \bar{y}$ plane. The unknown angle can be found by setting to zero the derivative with respect to γ of

$$H_h = H_{\bar{x}} \cos\gamma + H_{\bar{y}} \sin\gamma \quad , \tag{12}$$

resulting in

$$\tan 2\gamma = \frac{2\,\mathrm{Re}(H_{\bar{y}}/H_{\bar{x}})}{1 - |H_{\bar{y}}/H_{\bar{x}}|^2} \quad . \tag{13}$$

From (13) and the trigometric half angle formulas, we are able to obtain an expression for Tan γ which enables us to determine the angle γ within π radians. Finally, artifically interchanging $H_{\bar{x}}$ and $H_{\bar{y}}$ in (13) whenever the former is smaller in magnitude than the latter enables us, after some ado, to keep track of the sign ambiguity in (12) and so resolve it.

Explicit expressions for the field components $H_{\bar{x}}$, $H_{\bar{y}}$, and $H_{\bar{z}}$, orientated along the axes of the cartesian coordinate system of figure 1, are obtained by applying well-known coordinate transformation formulas to the field components given by equations (1). The resulting formulation is lengthy and will not be reproduced here.

The magnetic field components (1) can be calculated independently of both ϑ and φ', this being the slowest computer operation, and then combined in a subsequent program to produce plots of the wave tilt versus the horizontal distance X (figure 1). Since the component calculation routine must have specified sequential values of ϑ', and since the spherical coordinate transformation requires both ϑ' and φ' to locate a point in the unrotated $(R, \bar{\vartheta}, \bar{\varphi})$ coordinate system, we need to determine a relationship which will enable us to obtain φ' as a function of ϑ', ϑ, and ψ if we are to hold constant the dipole tilt angle θ and the azimuthal bearing angle ψ when plotting wave tilt versus X. From simple geometrical relationships in figure (1) we have the law of cosines,

$$X^2 = (R\sin\bar{\theta})^2 + (R_o\sin\theta)^2 + 2(R\sin\bar{\theta})(R_o\sin\theta)\cos\bar{\phi} \quad , \tag{14}$$

and the law of sines,

$$\frac{R\sin\bar{\theta}}{\sin\psi} = \frac{X}{\sin\bar{\phi}} \quad ,$$

from which we obtain

$$\sin\theta'\cos\varphi' = \Big\{\cos\gamma\sqrt{(1-\sin^2\vartheta\sin^2\gamma)\sin^2\vartheta' - (\tfrac{R_o}{R} - \cos\theta')^2\sin^2\vartheta\sin^2\gamma} - (\tfrac{R_o}{R} - \cos\theta')\sin\vartheta\cos\vartheta\sin^2\gamma\Big\}\Big/(1-\sin^2\vartheta\sin^2\gamma). \tag{15}$$

In utilizing (15) it is necessary to avoid specifying an angle θ' too small to meet the arc $\overset{\frown}{OB}$. The minimum angle ϑ_o' that can be used is obtained from

$$\sin\vartheta_o' = \sin\frac{\overset{\frown}{AB}}{R} \Big/ \sqrt{1 + \frac{1}{\tan^2\gamma\cos^2(\vartheta - \overset{\frown}{AB}/R)}} \quad . \tag{16}$$

Also, for angles $\psi > \frac{\pi}{2}$, for X to increase monotonicly the angle ϑ' must decrease from it's maximum value $\frac{\overset{\frown}{AB}}{R}$ to ϑ_o' and then start to increase. It is at this crossover point that the sign of the square root in (15) changes. Frequently ϑ_o' is less than the minimum angle ϑ' for which it is practical to sum the series to convergence, due to the extreme increase in the number of terms required when ϑ' is small. In 16, we have $\frac{\overset{\frown}{AB}}{R} = \vartheta - \sin^{-1}\left(\frac{R_o}{R}\sin\vartheta\right)$.

As previously mentioned, the ratio H of source depth to skin depth is an important problem parameter. Equally important is the ratio $\frac{d}{R}$, where

$$d = \sqrt{(R-R_o)^2 + 2RR_o\left(1 - \cos\frac{\overset{\frown}{AB}}{R}\right)} \quad .$$

The graphical results can be extrapolated to encompass any desired frequency, conductivity, sphere radius, or source depth by trade off from one parameter to another, as long as H and d/R are held constant.

A sample contour plot of the magnitude of the wave tilt function is given in figure 2, where the abscissa axis corresponds to the $\bar{y}$ axis and the ordinate axis corresponds to the $\bar{x}$ axis, the origin locating the point of intersection of the magnetic dipole current moment. Both coordinates are normalized with respect to the source depth, d. Here, $d \approx 100$ m, the sphere radius is 400 m, and the dipole tilt angle $\theta = 20°$. It is apparent in figure 2 that a great deal of symmetry exists about the current moment axis, leading to the conclusion that wave tilt measurements can lead to a determination of the source location.

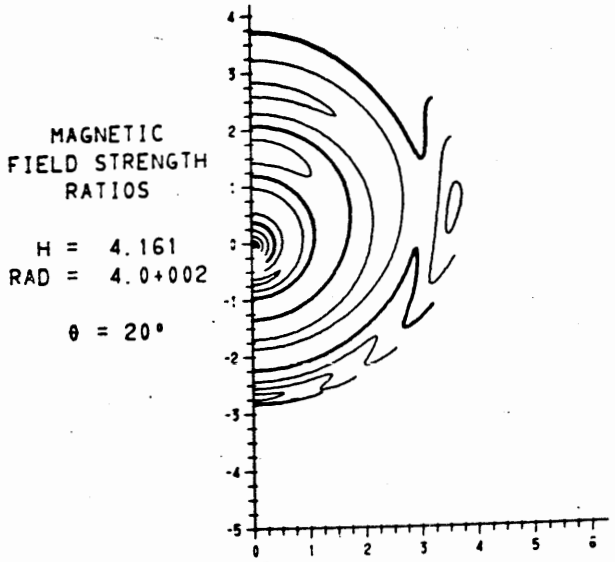

Figure 2. Wave tilt contours.

Figure 3 shows a plot of the amplitude of the wave tilt as a function of X/d, parametric in sphere radius (curve numbering refers to the increasing values of R) but with H held nearly constant ($R-R_o = 100$ m in figure 3). We can conclude that the wave tilt amplitude is nearly independent of sphere radius close in to the current moment axis, which in itself is a necessary requirement for a reliable source location scheme.

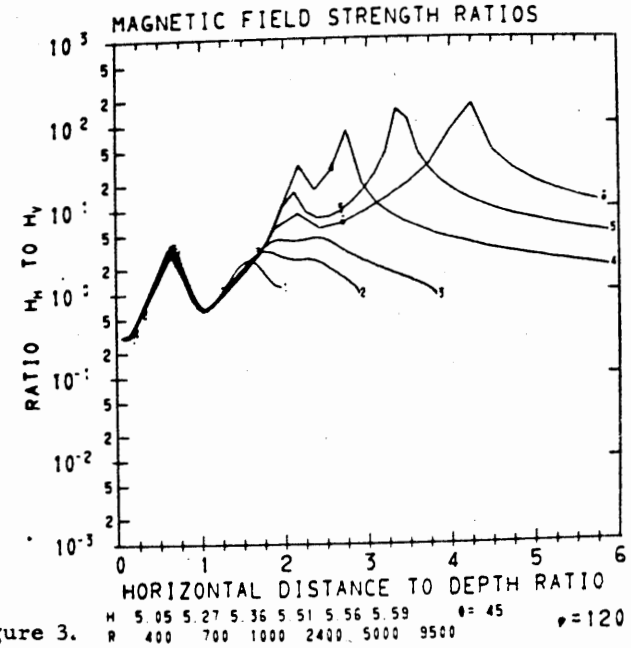

Figure 3.

A comparison of the numerical results for a spherical hill with an analysis by J. R. Wait[6] for the homogenous half-space leads to the conclusion that the amplitude of the wave-tilt function in both analyses is capable of providing useful information for electromagnetic position determination, but in the case of the spherical hill the phase of the wave-tilt function must be considered unreliable for this purpose.

Stratified Ionosphere Model

The second problem of interest is the stratified ionosphere problem of figure (4). Here it is assumed that the source is located at a radius r = b, while the observation point is at radius r. The formal problem solution, obtained by requiring continuity of the tangential fields at each spherical boundary, is a straightforward procedure.[3] The result is considerably simplified if it is specified that $k_1 = k_o$, which results in $R_1 = T = 0$ and $U_1 = -1$. Thus, we obtain, for the case $r > b$, the vertical electric field component

$$E_r = \frac{I_o \ell \mu_o c}{4\pi k_i^2 r^2 b^2} \sum_{n=0}^{\infty} n(n+1)(2n+1) P_n(\cos\theta) \times \frac{(\psi_{1b} - R\zeta^{(2)}_{1b})(\zeta^{(2)}_{1r} - \Gamma_1 \psi_{1r})}{1 - R\Gamma_1} \quad (17)$$

The quantity Γ_1 is an effective ionosphere reflection coefficient whose value is obtained as the end result of a recursion process,

$$\Gamma_j = \left[\frac{(1 - R_{2j}T_{2j}) - (R_{2j+1} - R_{2j}U_{2j+1})\Gamma_{j+1}}{(T_{2j-1} - U_{2j}T_{2j}) - (T_{2j-1}R_{2j+1} - U_{2j}U_{2j+1})\Gamma_{j+1}} \right]^{-1}, \quad (18)$$

for $j = 1, 2, \ldots, [\frac{p}{2}]$. The initial value for the recursion process is

$$\Gamma_{[\frac{p}{2}]+1} = \begin{cases} T_p & , \text{ p odd} \\ 0 & , \text{ p even} \end{cases} . \quad (19)$$

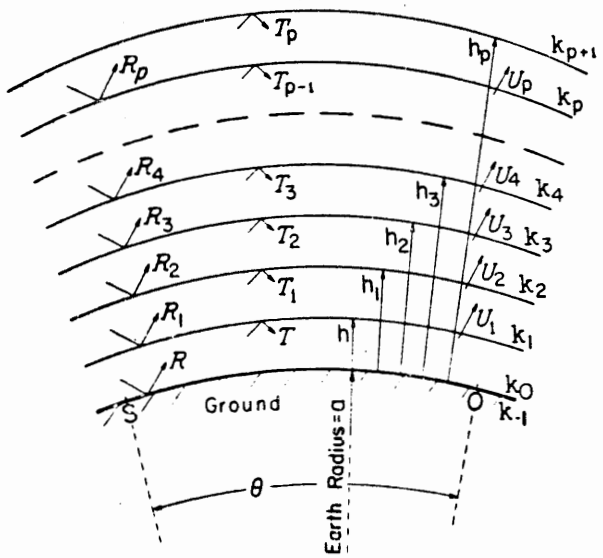

Fig. 4 Stratified ionosphere model of earth-ionosphere waveguide.

Figure (4) suggests the interpretation of R_j and T_j as the bottom and top reflection coefficients, respectively, of the j^{th} layer, while U_j has the character of a transmission coefficient for interlayer coupling. Replacing the spherical Bessel functions in R_j and T_j by the asymptotic expansions for large argument results in the Fresnel reflection coefficients[7] multiplied times a spherical focusing factor. The specific expressions are

$$R_j = \frac{-\psi_{jg_{j-1}}}{\zeta^{(2)}_{jg_{j-1}}} \frac{\frac{\psi'_{jg_{j-1}}}{\psi_{jg_{j-1}}} - \frac{k_j}{k_{j-1}} \frac{\psi'_{j-1g_{j-1}}}{\psi_{j-1g_{j-1}}}}{\frac{k_j}{k_{j-1}} \frac{\psi'_{j-1g_{j-1}}}{\psi_{j-1g_{j-1}}} - \frac{\zeta^{(2)'}_{jg_{j-1}}}{\zeta^{(2)}_{jg_{j-1}}}} \qquad T_j = \frac{-\zeta^{(2)}_{jg_j}}{\psi_{jg_j}} \frac{\frac{\zeta^{(2)'}_{jg_j}}{\zeta^{(2)}_{jg_j}} - \frac{k_j}{k_{j+1}} \frac{\zeta^{(2)'}_{j+1g_j}}{\zeta^{(2)}_{j+1g_j}}}{\frac{k_j}{k_{j+1}} \frac{\zeta^{(2)'}_{j+1g_j}}{\zeta^{(2)}_{j+1g_j}} - \frac{\psi'_{jg_j}}{\psi_{jg_j}}}$$

$$U_j = \frac{-\zeta^{(2)}_{j-1g_{j-1}}}{\psi_{j-1g_{j-1}}} \frac{\psi_{jg_{j-1}}}{\zeta^{(2)}_{jg_{j-1}}} \frac{\frac{\zeta^{(2)'}_{j-1g_{j-1}}}{\zeta^{(2)}_{j-1g_{j-1}}} - \frac{k_{j-1}}{k_j} \frac{\psi'_{jg_{j-1}}}{\psi_{jg_{j-1}}}}{\frac{k_{j-1}}{k_j} \frac{\zeta^{(2)'}_{jg_{j-1}}}{\zeta^{(2)}_{jg_{j-1}}} - \frac{\psi'_{j-1g_{j-1}}}{\psi_{j-1g_{j-1}}}} \quad . \qquad (20)$$

In (17) and (20) we have utilized the notation $\zeta^{(2)}_{jr} = \zeta^{(2)}_n(k_j r)$, $\psi_{jr} = \psi_n(k_j r)$, $\zeta^{(2)'}_{jr} = \zeta^{(2)'}_n(k_j r)$, $g_j = a + h_j$. Finally, we have the ground reflection coefficient

$$R = -\frac{\psi_{1a}}{\zeta^{(2)}_{1a}} \times \frac{\frac{\psi'_{1a}}{\psi_{1a}} - \frac{k_0}{k_{-1}} \frac{\psi'_{-1a}}{\psi_{-1a}}}{\frac{\zeta^{(2)'}_{1a}}{\zeta^{(2)}_{1a}} + \frac{k_0}{k_{-1}} \frac{\psi'_{-1a}}{\psi_{-1a}}} \quad , \qquad (21)$$

Calculation of the special functions involved in this formulation and use of the technique for grouping of terms to improve convergence proceeds in the same manner as for the spherical hill problem. Identical remarks also apply regarding the number of terms required for convergence and regarding which terms make the maximum contribution to the summation. An additional technique that is particularly useful in improving the series convergence properties is to subtract, term by term, the series expansion of the quasi-static fields of a dipole source near a perfectly conducting sphere from the summation (17).[3] The asymptotic expansion of each term in (17), for n large, can be shown to equal the corresponding term of the quasi-static series expansion, with the result that the term-by-term subtraction introduces a convergence factor of $\frac{1}{n}$ into the series summation. The quasi-static fields can be added back in at the end as a closed form expression. One note of caution regarding the truncation of the infinite series applies to the calculation of the phase correction term. This is defined as

$$\varphi_c = -\psi_r - k_1 d \quad , \qquad (22)$$

where $\psi_r = \arg\{E_r\}$ and $d = a\theta$. Since (22) is the difference of two very nearly equal terms (ψ_r is negative), practical experience has dictated that the accurate calculation of the phase correction may require roughly twice as many terms as is required to calculate the function amplitude.

In addition to the normal difficulties experienced in the calculation of spherical Bessel functions regarding underflow and overflow, there are also some particular problems associated with the formulation (17). Specifically, for the case b = a, we note that, for large n, $\frac{\zeta^{(2)}_{1a}}{\psi_{1a}} R \to 1$, assuming that the surface impedance of the earth is large. This machine underflow problem can be resolved by utilizing the Wronskian relation to obtain[2]

$$\psi_{1a} - R\,\zeta^{(2)}_{1a} = \frac{-i}{\zeta^{(2)'}_{1a} - \frac{k_0}{k_{-1}} \frac{\psi'_{-1a}}{\psi_{-1a}} \zeta^{(2)}_{1a}} \quad . \qquad (23)$$

Asymptotically it may be noted that (23) approaches zero for large n. Specific use may be made of this fact to improve the convergence properties of the series. Thus, we have [1,8]

$$\frac{\zeta^{(2)}_{1r} - \Gamma_1 \psi_{1r}}{1 - \Gamma_1 R} = \zeta^{(2)}_{1r} - (\psi_{1r} - R\,\zeta^{(2)}_{1r}) \sum_{j=1}^{\infty} R^{j-1} \Gamma_1^j \quad . \qquad (24)$$

Upon substitution of the first term in (24) into (17), there results simply the ground wave term, which can be calculated separately using the classical ground wave theory.[9] Interchanging the order of summation of j and n when the second term of (24) is substituted into (17) results in the wave-hop summation,[1] illustrated in figure (5). Here, the source is at S and the observer is at O. The usefulness of this technique arises from the fact that only a few wave-hops need be summed for reasonable accuracy, while we have introduced the additional factor $\psi_{1r} - R\,\zeta^{(2)}_{1r}$ which can be treated in similar fashion to (23). Thus, only a few terms beyond $n \approx k_1 a$ need be summed for the summation over n to converge.[2] This technique is used at VLF and LF frequencies.

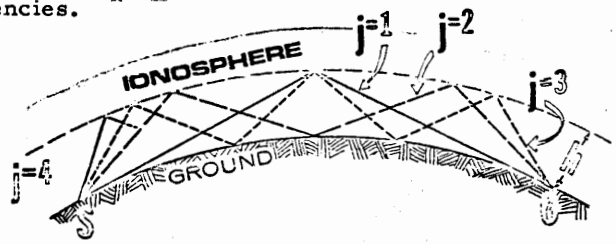

Figure 5. The wave hop fields.

An example of the capability of the formulation is depicted in figure 6, where we show the complicated field

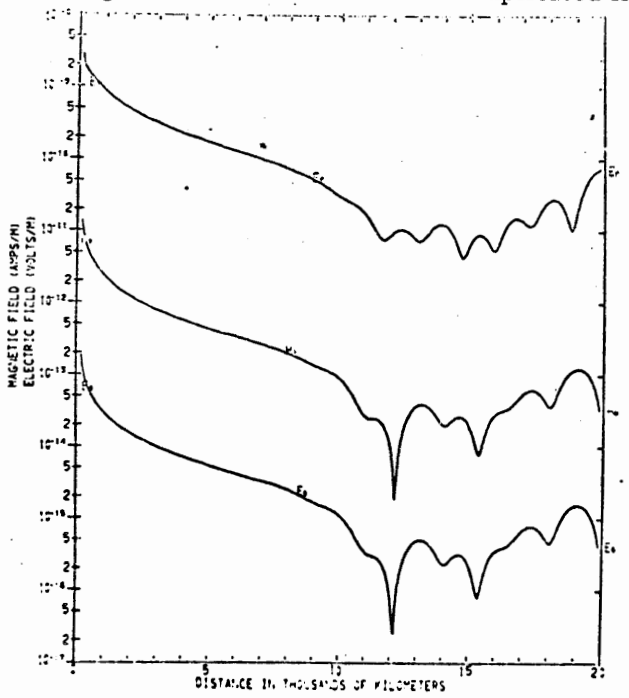

Fig. 6. Two layer ionosphere with low conductivity bottom layer.

structure produced by a two layer ionosphere in which the upper layer has a very high conductivity while the lower layer is a moderately lossey dielectric. Thus, the two layer "ionosphere" functions as a dielectric coated conducter which guides a surface wave completely around the spherical wave-guide, leading to the standing-wave pattern shown. The upper trace is the E_r field, while below that are the H_ϕ and $E\theta$ fields. The lowest layer, at a height of 70 km, was taken to be $1\frac{1}{2}$ km thick, while the excitation frequency is 100 Hz.

In figure 7, we show the effect of increasing the conductivity of the lowest layer by an order of magnitude. Here, the standing wave structure is greatly enhanced. Finally, in figure 8, we have decreased the conductivity of the lowest layer by an order of magnitude from the value used in figure 6. Figure 8, incidentally, is identical with the result obtained for a single layer or sharply bounded ionosphere commonly used when the conductivity of lower layers is simply ignored.

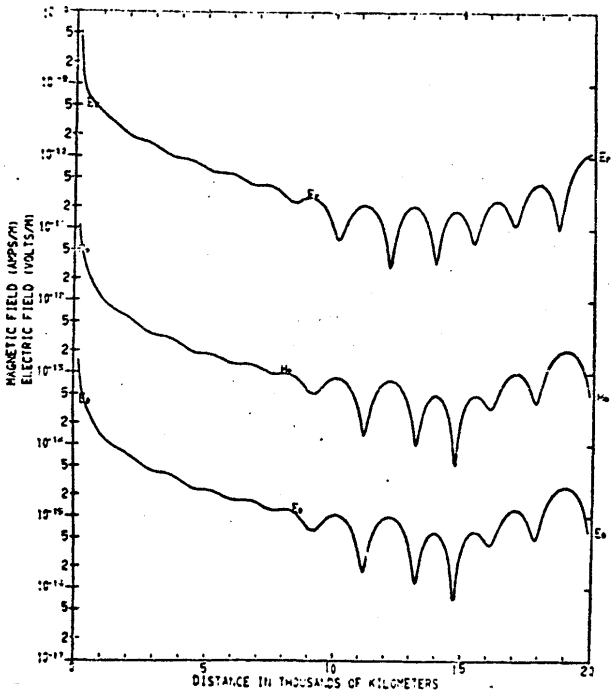

Fig. 7. Two layer ionosphere with moderate conductivity bottom layer.

In conclusion, it might be worthwhile to contrast the zonal-harmonic series summation with the more convential mode theory approach. Although either formulation is equally valid, it must be noted that the latter approach requires a time consuming search for modes, possibly involving a very complicated modal equation. Especially this would be true for the treatment of a spherically layered model. Furthermore, it should be pointed out that more than one mode may be required to fully explain a complicated field structure such as is shown in figure 6, even at the low frequency of 100 Hz. Consequently, although the determination of the field strength can proceed extremely rapidly once the modes are known, I submit that the necessary mode determination could be a detering factor from considering a mode theory approach. The zonal-harmonics summation, on the other hand, can be extremely rapid, particularly when $|k_1 a|$ is not too large, although some physical insight may be sacrified by it's use.

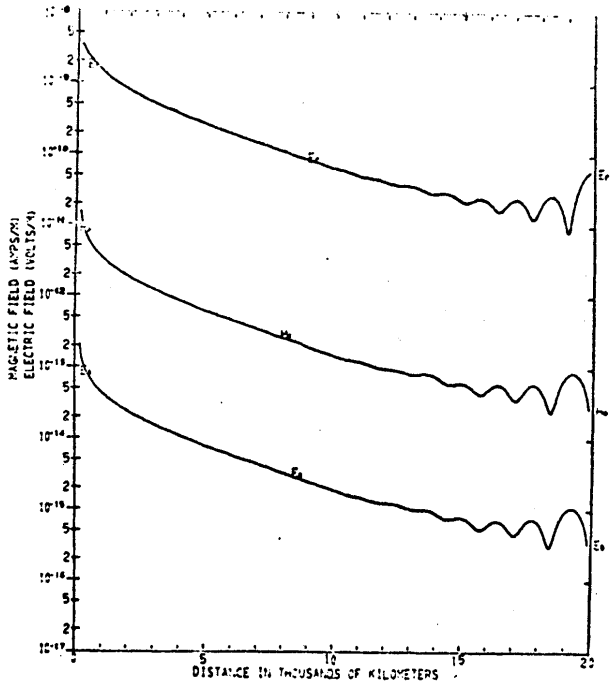

Fig. 8. Two layer ionosphere with extremely low conductivity bottom layer.

[1]Richard L. Lewis, "The wave-hop fields for an inclined dipole over a spherical earth with an anisotropic ionosphere", Telecommunication Research Report OT/ITS 5, U.S. Dept. of Commerce, Oct. 1970.

[2]J. Ralph Johler, "Spherical wave theory for MF, LF, and VLF propagation", Radio Science 5, 12, pp. 1429-1443, Dec. 1970.

[3]J. Ralph Johler and Richard L. Lewis, "Extra low-frequency terrestrial radio-wave field calculations with the zonal-harmonic series", Journal of Geophysical Research 74, 10, pp. 2459-2470, May 15, 1969.

[4]Walter Gautschi, "Computational Aspects of Three-Term Recurrence Relations," SIAM Review 9, 1, pp. 24-82, January 1967.

[5]Richard L. Lewis, "Recursion Formula for the Logarithmic Derivatives of Spherical Bessel Functions in the Complex Plane", ESSA Technical Report ERL 151-ITS 99, U. S. Dept. of Commerce, January 1970.

[6]J. R. Wait, "Electromagnetic Sources in Lossy Media," Chapter 24 in Antenna Theory, pt. II, Ed. by Collin & Zucker, McGraw Hill 1969, cf. also: J. R. Wait, "Influence of earth's curvature on the subsurface fields of a line source," Electronics Letters 7, 23, pp. 697-699, Nov. 1971.

[7]J. R. Wait, Electromagnetic Waves in Stratified Media, Pergamon Press 1970, c.f. also: J. Ralph Johler, "Zonal harmonics in low frequency terrestrial radio wave propagation, NBS Tech note 335, U. S. Dept. of Commerce, April 13, 1966.

[8]J. Ralph Johler, "Concerning limitations and further corrections to geometric-optical theory for LF, VLF propagation between the ionosphere and the ground.", Radio Science 68D, 1, pp. 67-78, January 1964.

[9]Johler, J. R., and J. C. Morgenstern, "Propagation of the ground wave electromagnetic signal with particular reference to a pulse of nuclear origin", Proc. IEEE 53, 12, pp. 2043-2053, 1965.